

Search for Correlations between Nearby AGNs and Ultra-high Energy Cosmic Rays

J. D. Hague^a J.A.J. Matthews^{a,1} B. R. Becker^a M. S. Gold^a

^a*University of New Mexico, Department of Physics and Astronomy, Albuquerque, New Mexico, USA*

Abstract

The majority of the highest energy cosmic rays are thought to be electrically charged: protons or nuclei. Charged particles experience angular deflections as they pass through galactic and extra-galactic magnetic fields. As a consequence correlation of cosmic ray arrival directions with potential sources has proved to be difficult. This situation is not helped by current data samples where the number of cosmic rays/source are typically $\leq O(1)$. Progress will be made when there are significantly larger data samples and perhaps with better catalogs of candidate sources. This paper reports a search for correlations between the RXTE catalog of nearby active galactic nuclei, AGNs, and the published list of ultra-high energy cosmic rays from the AGASA experiment. Although no statistically significant correlations were found, two correlations were observed between AGASA events and the most inclusive category of RXTE AGNs.

Key words: highest energy cosmic rays – AGNs as sources – search for correlations

1 Introduction

Perhaps the primary goal of all experiments studying the highest energy cosmic rays is to find the source of these particles. While circumstantial evidence may favor one type of source over another, demonstration of a clear correlation between the direction of cosmic rays and their sources is arguably essential. Unfortunately for electrically charged cosmic rays, galactic magnetic fields, and for the highest energy cosmic rays extra-galactic magnetic fields, cause angular deflections that can blur the correlation between cosmic ray arrival

¹ Corresponding author, E-mail: johnm@phys.unm.edu

direction and source direction. If the sources as viewed from the earth are extended [1,2] the problem is even more difficult. Unless otherwise noted, for this paper we assume compact (point-like) sources for the highest energy cosmic rays.

If the angular blurring from magnetic fields is small [3] (*i.e.* not significantly greater than the experimental angular resolution) and/or for neutral primaries, then experiments should observe cosmic rays that cluster in arrival direction [4,5], and/or that correlate with potential astronomical (*e.g.* BL Lac) sources [6–10]. For nearby sources, where experiments should detect multiple cosmic rays/source, event clusters provide bounds on the cosmic ray source density [11–13] potentially favoring one type of source for the highest energy cosmic rays over another. However at this time the situation is less than clear as some results [14,15] question the significance of the reported clusters and/or some of the BL Lac correlations [10,16].

If deflections of charged cosmic rays by extra-galactic magnetic fields are not small [17], then lower energy, E , cosmic rays should experience the greatest angular deflections. Unfortunately small experiment data samples and a cosmic ray flux $\propto E^{-3}$ have often caused studies to retain cosmic rays to energies, E_{thresh} , well below GZK [18] energies [4]. Furthermore deflections of the highest energy cosmic rays even by our galactic magnetic field can be substantial [19–21]. As magnetic deflections scale proportional to the charge of the primary cosmic ray, nuclei in the cosmic rays may have significant deflections. Although most searches have looked for clustering and/or source correlations on small angular scales, studies at larger angular scales have also found evidence for clustering and/or source correlations [22–24]. Certainly the angular scale of cosmic ray clusters and the magnitude, and thus relevance, of the deflections of ultra-high energy cosmic rays by magnetic fields is not universally agreed to at this time.

In the future, significantly larger data samples will allow analyses to increase E_{thresh} while retaining the number of observed cosmic rays/source (for nearby sources) $\geq O(1)$. However another possibility is to exploit catalogs of candidate sources. With a catalog of source directions, cosmic rays can be effectively correlated with sources even when magnetic field deflections are “not small” and/or when the number of observed cosmic rays per source is < 1 allowing searches with existing data samples. That said, catalog based studies are limited by the completeness of the source catalog and the relevance (or not) of that class of astronomical source to the production of the highest energy cosmic rays. Often conjectured astrophysical sources include gamma ray bursts, GRBs, and/or active galactic nuclei, AGNs [25].

This paper reports a search for correlations between a catalog of nearby AGNs [26] and the published list of ultra-high energy cosmic rays from AGASA [4].

The components of our analysis are listed in Section 2. Issues that relate to data and AGN selection are given in Section 3. The cosmic ray–AGN comparison results are given in Section 4. Section 5 summarizes this study.

2 Analysis Components

Our comparison of ultra-high energy cosmic rays and a catalog of AGNs includes three components: the RXTE catalog of AGNs, the AGASA list of cosmic rays, and a Monte Carlo sample of uniformly distributed cosmic rays generated to match the experimental acceptance of AGASA.

The catalog of nearby AGNs [26] results from the Rossi X-ray Timing Explorer, RXTE, all-sky slew survey [27] sensitive to sources of hard X-rays (3–20 keV). The survey excluded the galactic plane ($|b| > 10^\circ$) but covered $\sim 90\%$ of the remaining sky. X-ray sources were located to better than 1° and then correlated with known astronomical objects. The efficiency for AGN identification was estimated to be $\sim 70\%$ with somewhat higher efficiency for northern AGNs ($\sim 87\%$) and somewhat lower efficiency for southern AGNs ($\sim 60\%$) [26]. The resulting catalog provides source directions and probable source distances and intrinsic X-ray luminosities, L_{3-20} . The catalog is best for nearby AGNs as RXTE signal thresholds significantly reduced the efficiency for detecting distant sources; additional details are given below.

The list of ultra-high energy cosmic rays comes from published AGASA data [4].

The Monte Carlo sample of uniformly distributed cosmic rays was generated according to a $\cos(\theta)\sin(\theta)$ distribution in local zenith angle, $\theta \leq 45^\circ$, and uniform in local azimuth. Events were then transformed to celestial right ascension and declination assuming constant detector aperture with time.

Correlations, between the AGASA events and the catalog of AGNs from RXTE, would appear as an excess at small angular separations in comparison to the Monte Carlo sample of simulated cosmic rays. To be clear, define unit vectors in the directions of cosmic rays, \hat{u}_i , AGNs, \hat{v}_j , and Monte Carlo simulated cosmic rays, \hat{w}_k . A correlation *signal* should then appear *near 1.0* in the distribution of *dot*-products: $\hat{u}_i \cdot \hat{v}_j$ (if magnetic field deflections are modest). The index “*i*” runs over the cosmic rays in the data sample. For each value of “*i*”, only the AGN catalog source (index “*j*”) giving the maximum value of: $\hat{u}_i \cdot \hat{v}_j$ contributes to the distribution². The simulated distribution of *random background* comes from the analogous distribution of: $\hat{w}_k \cdot \hat{v}_j$ where

² Thus each cosmic ray has one entry in the *dot*-product distribution. This choice is consistent with each cosmic ray having one source. As only the AGN source *nearest*

index “ k ” now runs over the sample of Monte Carlo simulated cosmic rays. As with the cosmic ray events, only the AGN catalog source (index “ j ”) giving the maximum value of: $\hat{w}_k \cdot \hat{v}_j$ contributes to the distribution.

3 Cosmic Ray and AGN Selection

A few choices have been made in the comparison of AGASA data and catalog of AGNs from RXTE. These are described here.

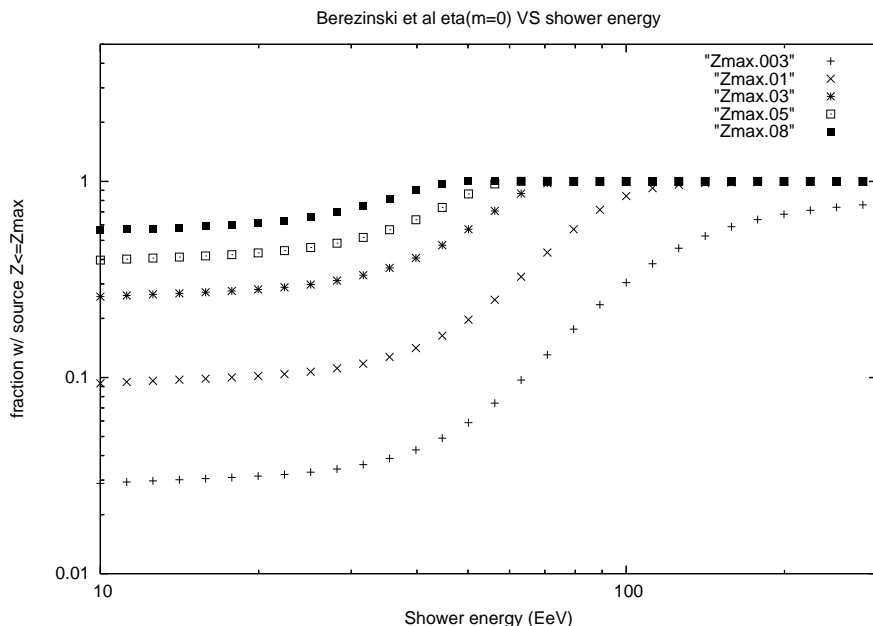


Fig. 1. The curves, from a GZK model [28], show the predicted fraction of cosmic ray events with source redshift, $z < z_{max}$ versus cosmic ray energy for a selection of z_{max} distances: $0.003 \leq z_{max} \leq 0.08$. The GZK model assumed proton primaries with a power law spectrum at the source $\propto E^{-2.7}$. No enhancement factor of increasing source density with redshift, z , was included. The result was derived from Fig.6 of Ref. [28].

The AGASA data have energies, $E > 40\text{EeV}$ and populate values of declination: $-10^\circ \leq Dec \leq 80^\circ$. As noted above, the steep cosmic rays spectrum, $\propto E^{-3}$, and modest number of events: 57 with $E > 40\text{EeV}$ and 29 (just over half) with $E > 53\text{EeV}$ led us to consider three (overlapping) bins in energy: $E \geq 40\text{EeV}$, $E \geq 53\text{EeV}$ and $E \geq 100\text{EeV}$. The last was to see if there are any correlations with the AGASA super-GZK events. Except for the $E \geq 100\text{EeV}$

in angle to the cosmic ray is chosen this can result in possible misidentification in the case of large source density.

selection, most of the cosmic rays are predicted, at least under the assumption of proton primaries [28], to originate at values of redshift, $z > 0.01$ ³; see Fig. 1.

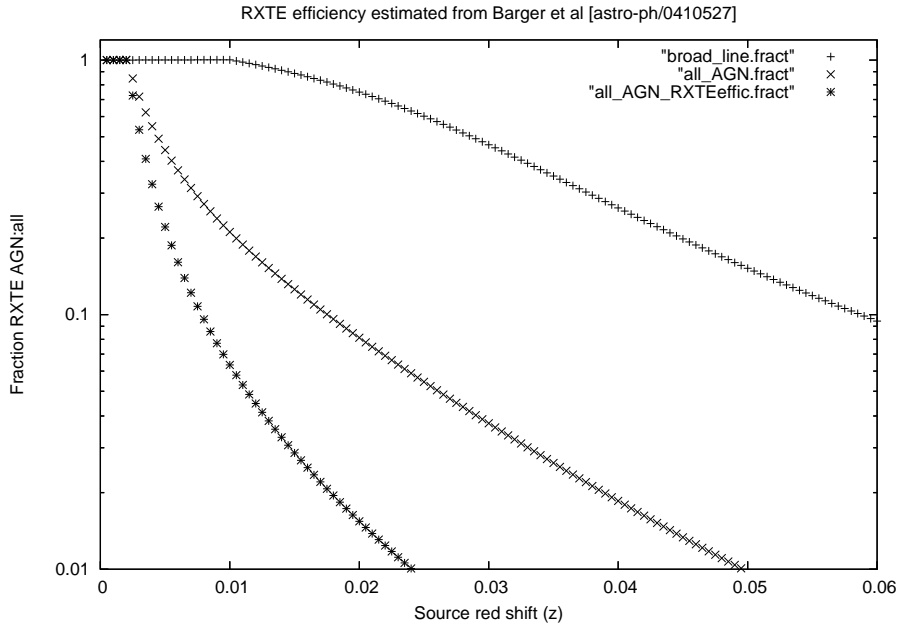


Fig. 2. The curves show the estimated RXTE source detection efficiency, *i.e.* the fraction of RXTE AGNs [26] to all AGNs [30], *VS* source distance resulting from the RXTE instrument detection threshold. As noted in the text, two categories (or definitions) of AGNs are considered: *all*-AGNs with RXTE 3-20keV intrinsic luminosities, $L_{3-20} \geq 10^{41}$ ergs/s shown as “x”, and *broadline*-AGNs with 2-8keV intrinsic luminosities, $L_{2-8} \geq 10^{42}$ ergs/s shown as “+”. For redshift (distances) with full RXTE source detection efficiency then the fraction is 1. Parenthetically, we would obtain lower efficiencies (for the *all*-AGN category) if we were to use the AGN number density *VS* X-ray luminosity deduced by the RXTE experiment [26] and shown as “*”.

To match the AGASA acceptance, we selected AGNs with $-10^\circ \leq Dec \leq 80^\circ$. We have also made selections on the redshift of the AGNs to consider sources only with RXTE source detection efficiency $\gtrsim 50\%$.

The estimate of the RXTE source detection efficiency involves two issues:

- (1) the RXTE instrument source detection threshold (*i.e.* the selection bias) *VS* redshift from Fig.1 of Ref. [26],
- (2) the number density of AGNs *VS* redshift and intrinsic X-ray luminosity from Table 2 of Ref. [30].

Motivated by Ref. [30], we divide the AGNs into the two categories: *all*-AGNs

³ This corresponds to a distance $r \approx 42$ Mpc

and *broadline*-AGNs. For the *all*-AGN category we require that the X-ray 3-20keV intrinsic luminosity ⁴, $L_{3-20} \geq 10^{41}$ ergs/s, to match the RXTE data. With this intrinsic luminosity threshold the estimated *all*-AGN number density is $4.2 \times 10^{-4} \text{ Mpc}^{-3}$ consistent with the RXTE source density determination of $\sim 5 \times 10^{-4} \text{ Mpc}^{-3}$ [26]. For the *broadline*-AGN category we require that the X-ray 2-8keV intrinsic luminosity, $L_{2-8} \geq 10^{42}$ ergs/s as this selects X-ray sources that are likely to be AGNs based purely on energetic grounds [29]. With this intrinsic luminosity threshold the estimated *broadline*-AGN number density is $\sim 2 \times 10^{-5} \text{ Mpc}^{-3}$.

Combining the RXTE detection threshold with our definition of two categories of AGN (above), we obtain the fraction of each AGN category *VS* redshift. This is shown in Fig. 2. Based on this result we restrict the redshifts for the *all*-AGN category to $z \leq 0.005$ and the redshifts for the *broadline*-AGN category to $z \leq 0.03$.

4 Cosmic Ray–AGN Comparisons

Plots of the distribution of *dot*-products (see definition in text) for the *all*-AGN selection are shown in Fig. 3. A plot of the AGASA cosmic ray and RXTE AGN directions are given in Fig. 4. The analogous plots for the *broadline*-AGN selection are shown in Fig. 5 and 6. A comparison of Figs. 4 and 6, shows two events shared between the two selections. Independently we have verified that all RXTE AGNs with redshift $z \leq 0.03$ satisfy at least one of our two AGN categories.

The plots of the *dot*-products for the *all*-AGN selection, Fig. 3, shows a small excess in the bin nearest to 1 for the AGASA event selections $E \geq 40\text{EeV}$, and $E \geq 53\text{EeV}$. For this bin (*i.e.* *dot*-product ≥ 0.975) the excesses are ~ 1.1 and ~ 1.7 standard deviations for the AGASA event selections $E \geq 40\text{EeV}$, and $E \geq 53\text{EeV}$ respectively. If this correlation is valid, then it could provide experimental information to bound the magnetic deflections of extra-galactic cosmic rays.

To see if the *all*-AGN category excesses are consistent with *e.g.* typical GZK models, see Fig. 1, we estimate the RXTE AGN catalog efficiency as follows:

- (1) 90% sky coverage of the $\sim 83\%$ of the sky surveyed ⁵;

⁴ For our study we relate the RXTE 3-20keV intrinsic luminosities, L_{3-20} in ergs/s, to 2-8keV intrinsic luminosities, L_{2-8} in ergs/s using: $L_{2-8} \approx L_{3-20}/2$; private communication from Sergey Sazonov.

⁵ This corresponds to the sky fraction outside a 10° avoidance zone about the galactic plane

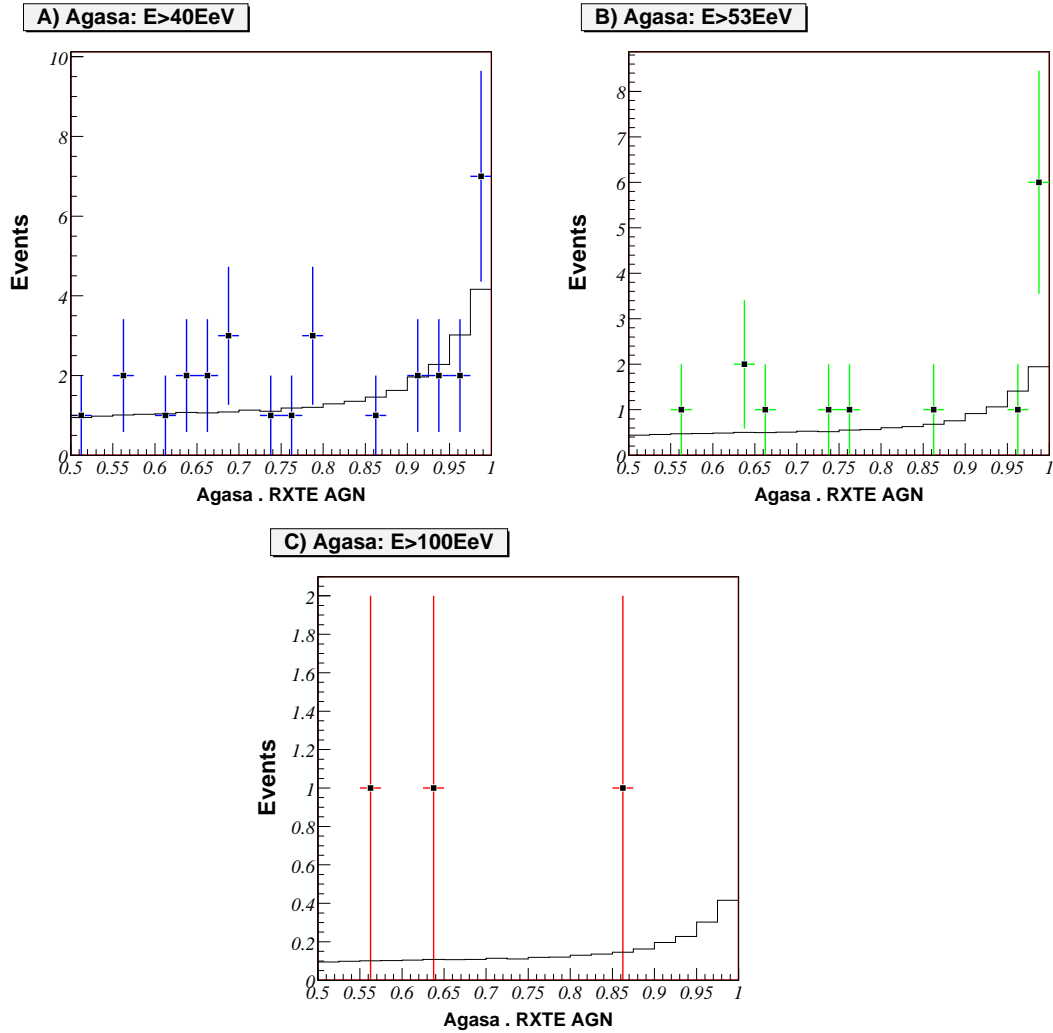


Fig. 3. The plots show the distribution of *dot*-products (see definition in the text) for the *all*-AGN selection: (top left) with cosmic ray energies $E \geq 40\text{EeV}$, (top right) with cosmic ray energies $E \geq 53\text{EeV}$, and (bottom) with cosmic ray energies $E \geq 100\text{EeV}$. The curve on each figure shows the Monte Carlo *random background* normalized to the number of entries in each plot.

- (2) 87% estimated completeness factor;
- (3) $\sim 77\%$ estimated average *all*-AGN source detection efficiency (from Fig. 2).

This yields an lower bound estimate for the *all*-AGN RXTE efficiency of $\sim 50\%$. However for the *all*-AGN category (only 5 sources, see Fig. 4) it is likely that the global (redshift independent) RXTE efficiency factors are not appropriate⁶. To obtain an upper bound estimate for the *all*-AGN RXTE ef-

⁶ In particular assuming an average AGN source density of $4.2 \times 10^{-4} \text{ Mpc}^{-3}$ (see above) and the RXTE global efficiency [26] of $0.9 \times 0.83 \times 0.7 \approx 52\%$, the predicted number of nearby ($z \leq 0.005$) RXTE AGNs is approximated half those observed. While the small number of AGNs makes this weak statistically, it is nevertheless

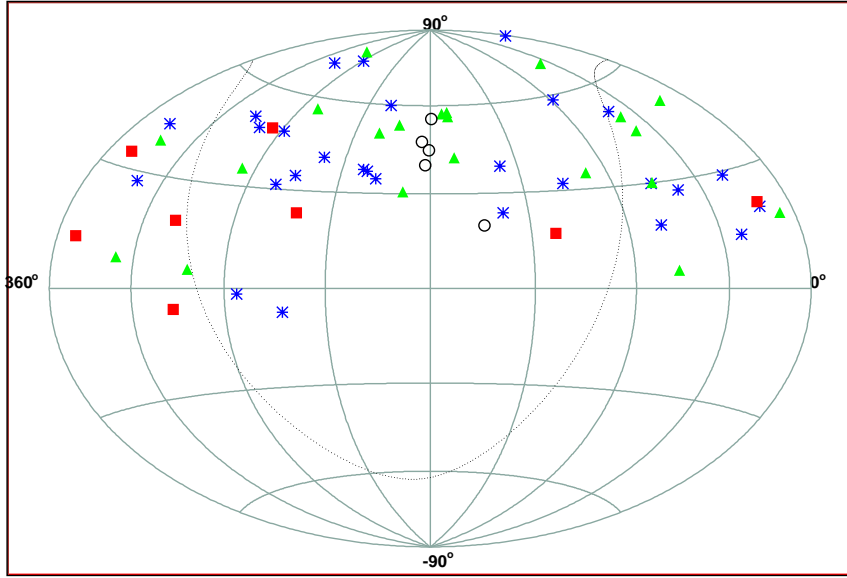


Fig. 4. The figure shows the map of $RA - Dec$ for the AGASA data and the AGNs from the *all*-AGN selection. The AGASA data are plotted in *blue*(*) for $40\text{EeV} \leq E < 53\text{EeV}$, *green*(\blacktriangledown) for $53\text{EeV} \leq E < 100\text{EeV}$, and *red*(\blacksquare) for $100\text{EeV} \leq E$. The RXTE AGNs are plotted as *black*(\circ). The galactic plane is drawn as a dotted line.

efficiency we assume the global RXTE efficiency is $\sim 100\%$. Then the estimated (upper bound) *all*-AGN RXTE efficiency is $\sim 77\%$.

The estimated number of cosmic ray:*all*-AGN coincidences is: the number of cosmic rays (with sources in a given redshift region) times the average *all*-AGN source detection efficiency (for the same redshift region). Thus the estimated number of cosmic rays from the $z < 0.005$ region is obtained by dividing the excess counts, Fig. 3, by the *all*-AGN efficiencies to obtain: $2.8/0.77 \sim 2.8/0.50$ or $3.6 \sim 5.6$ events and $4.0/0.77 \sim 4.0/0.50$ or $5.2 \sim 8.0$ events respectively. As fractions of all the observed cosmic rays these are: $3.6 \sim 5.6/57$ (or $6.3 \sim 9.8\%$) and $5.2 \sim 8.0/29$ (or $18 \sim 28\%$) respectively. These fractions are somewhat, to significantly (depending on the *all*-AGN RXTE efficiency), in excess of typical GZK models assuming proton primaries, see Fig. 1.

Finally we note that the AGASA/HiRes cosmic ray *quartet* (or possibly *quin-*

consistent with: a RXTE global efficiency of $\sim 100\%$ for nearby ($z \leq 0.005$) AGNs and/or with a local over-density of AGNs. Although these estimates were based on the AGN number density *VS* X-ray luminosity from Ref. [30] the AGN number density *VS* X-ray luminosity deduced by the RXTE experiment [26] gave a similar result.

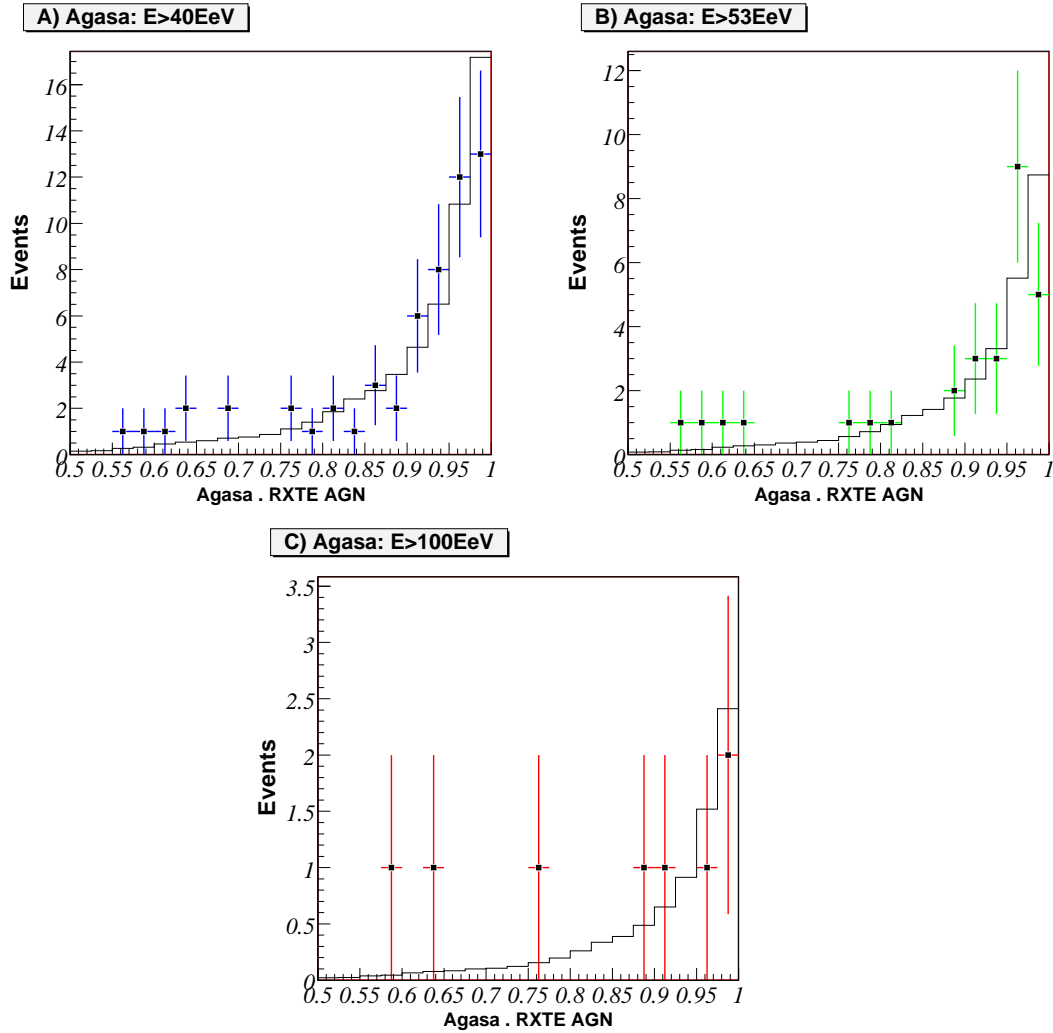


Fig. 5. The plots show the distribution of *dot-products* for the *broadline-AGN* selection: (top left) with cosmic ray energies $E \geq 40\text{EeV}$, (top right) with cosmic ray energies $E \geq 53\text{EeV}$, and (bottom) with cosmic ray energies $E \geq 100\text{EeV}$. The curve on each figure shows the Monte Carlo *random background* normalized to the number of entries in each plot.

tet[31]) cluster, at RA $\approx 169.1^\circ$, Dec $\approx 56.3^\circ$ [15], is near one of the the RXTE AGNs at: RA 179.3° , Dec 55.23° and redshift $z = 0.0035$. In contrast, there is no close correlation in the *all-AGN* selection with any of the AGASA super-GZK events [4] plotted in Fig. 4 (more below).

The plots of the *dot-products* for the *broadline-AGN* selection, Fig. 5, are consistent with *random background*. If we assume the cosmic rays are primarily protons, then we can use a model such as Fig. 1 to estimate the number of cosmic rays expected from sources with redshifts $z \leq 0.03$. Then *e.g.* for the AGASA selection $E \geq 53\text{EeV}$, we expect $\sim 60\%$ to originate from sources with redshifts $z \leq 0.03$ or ~ 17.4 events. However the number that should

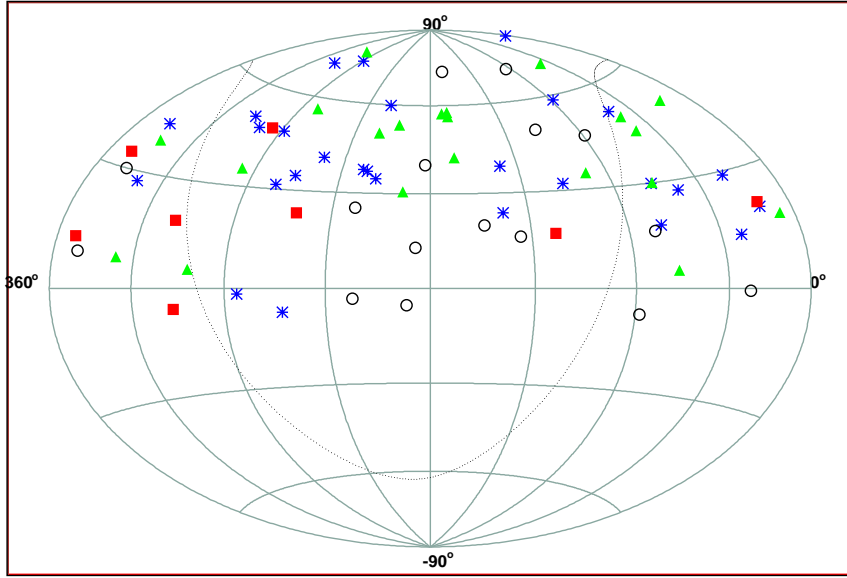


Fig. 6. The figure shows the map of $RA - Dec$ for the AGASA data and the AGNs from the *broadline*-AGN selection. The AGASA data are plotted in *blue*(*) for $40\text{EeV} \leq E < 53\text{EeV}$, *green*(\blacktriangledown) for $53\text{EeV} \leq E < 100\text{EeV}$, and *red*(\blacksquare) for $100\text{EeV} \leq E$. The RXTE AGNs are plotted as *black*(\circ). The galactic plane is drawn as a dotted line.

appear in *dot*-product bins near 1 depends on the RXTE AGN catalog efficiency. Similar to the evaluation above, we obtain an overall *broadline*-AGN RXTE efficiency of $\sim 54\%$. Thus we should observe a *signal* as an excess of ~ 9.4 events. Unfortunately in absence of a signal signature (*i.e. dot*-product bins in excess of *random background*) or of a bound on magnetic field deflections, any statement on lack of excess depends on the assumed *dot*-product range. That said, assuming any *signal* would appear at *dot*-products ≥ 0.95 then ~ 9.4 events should result in a ~ 1.9 standard deviation excess. With the AGASA statistics and our current knowledge of cosmic ray deflections by magnetic fields, no strong conclusion can be drawn.

The final issue is the evidence for, or against, correlations between the RXTE catalog of AGNs and the most energetic AGASA events. To investigate this, we show in Fig.7 all of the AGNs from the RXTE catalog with $z \leq 0.03$ and all of the AGASA events above 100EeV as updated on the AGASA web site [32]. Now with 11 super-GZK events: 3 have *dot*-products > 0.975 , ~ 3 are close to the galactic plane (region unobserved by RXTE) and the remaining 5 do not correlate well (*e.g. dot*-product $\lesssim 0.95$) with the RXTE catalog of AGNs.

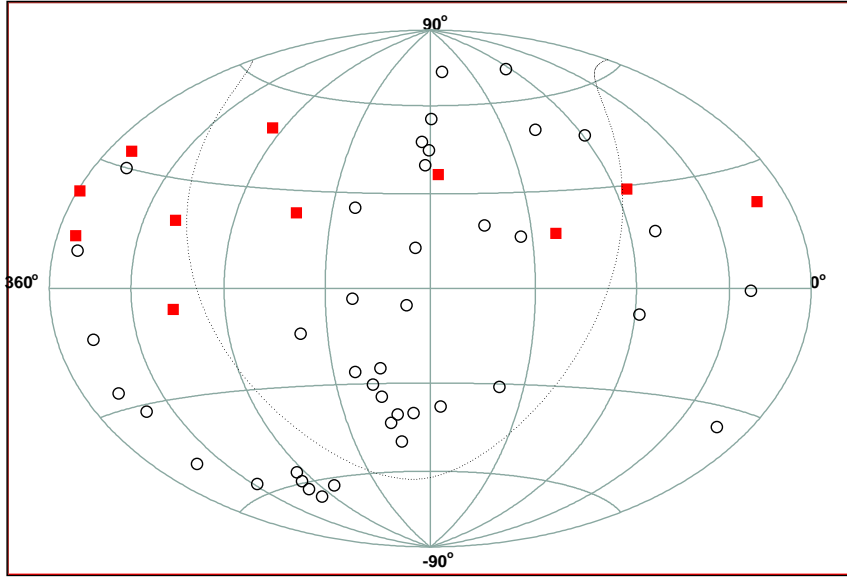


Fig. 7. The figure shows the map of $RA - Dec$ for the updated list [32] AGASA events with energies $E \geq 100\text{EeV}$ and the RXTE catalog of AGNs with redshift $z \leq 0.03$ without restriction on AGN declination. The AGASA events are plotted in *red*(■). The RXTE AGNs are plotted as *black*(○). The galactic plane is drawn as a dotted line.

While the 3 AGASA super-GZK events that are close to RXTE catalog AGNs are consistent with *random background*, on inspection these events all have *dot-products* > 0.99 . In this case the expected *random background* is ~ 1.6 . Furthermore one of these events, with energy $E = 122\text{EeV}$ and $RA\ 176.0^\circ$, $Dec\ 36.3^\circ$, is close to the group of very nearby ($z < 0.005$ in Fig. 4) AGNs. The closest correlation is with the RXTE AGN at: $RA\ 182.7^\circ$, $Dec\ 39.45^\circ$ and redshift $z = 0.0033$.

Of the 5 AGASA super-GZK events that do not correlate well with the RXTE AGNs, 4 lie far from the galactic plane and have energies well above 100EeV . Thus for proton primaries, based on Fig. 1 these should originate at redshifts $z \lesssim 0.01$. For the *broadline*-AGN category the RXTE average source detection efficiency is then $\sim 100\%$ based on Fig. 2. Thus for these AGASA events we expect $\sim 4 \times 0.9 \times 0.87 = 3.1$ correlations with the RXTE catalog of AGNs whereas we observe zero. Furthermore, the Poisson probability of then observing zero is small: 4.4%.

In contrast if the *all*-AGN category is the more appropriate source of super-GZK events, then the RXTE average source detection efficiency based on Fig. 2 is significantly less than 100%, particularly for source redshifts to $z \lesssim 0.01$. In

this case, the *all*-AGN category the RXTE average source detection efficiency is estimated at $\sim 53\%$, resulting in an overall RXTE catalog efficiency of $\sim 34\%$. Thus we expect approximately $11 \times 0.34 = 3.7$ correlations (with sources to $z \lesssim 0.01$). The Poisson probability to observe ≤ 1 correlation (one correlation was observed with the RXTE AGNs to $z \lesssim 0.01$) is 11.6% ⁷ However if the AGASA energies are overestimated (with respect to the energy scale of Fig. 1) then some of the AGASA events with energies closest to 100EeV could originate at redshifts $z > 0.01$. If we extend the possible RXTE AGNs to redshifts of $z \lesssim 0.02$ then the RXTE average source detection efficiency decreases to $\sim 33\%$ (because most of the lower X-ray luminosity AGNs are unobserved by RXTE) resulting in an overall RXTE catalog efficiency $\sim 21\%$. Thus we expect $11 \times 0.21 = 2.3$ correlations and we observe two. The (new) additional correlation is between an AGASA event with $E = 120\text{EeV}$ and a RXTE AGN at redshift $z = 0.016$. The Poisson probability to observe two correlations is $\sim 27\%$.

5 Summary

We have searched for correlations between the published list of the highest energy events from the AGASA experiment [4,32] and the RXTE catalog of AGNs [26]. Two categories of RXTE AGNs were considered: *all*-AGNs with RXTE 3-20keV intrinsic luminosities, $L_{3-20} \geq 10^{41}$ ergs/s, and *broadline*-AGNs with 2-8keV intrinsic luminosities, $L_{2-8} \geq 10^{42}$ ergs/s motivated by the analysis of AGN evolution in Ref. [30]. To retain RXTE source detection efficiencies $\gtrsim 50\%$, source redshifts of $z \leq 0.005$ and $z \leq 0.03$ were required for the *all*-AGN and *broadline*-AGN categories respectively.

No correlations were observed between the AGASA events and the *broadline*-AGN category of RXTE AGNs even though this category of AGN is most luminous in X-rays and even though the source density for this category of AGN is favored by some analyses [12,13] of the highest energy cosmic rays.

In contrast, possible correlations were observed between AGASA events and the most inclusive, *all*-AGN, category of RXTE AGNs. We note that while not statistically conclusive, one of the nearby RXTE AGNs correlates with the AGASA/HiRes *quartet* event cluster [15] and one correlates with one of

⁷ If we also include the 320EeV event from the Fly's Eye [33] then we expect $12 \times 0.34 = 4.08$ correlations (with RXTE AGNs to $z \lesssim 0.01$) and we observe one. Now the Poisson probability to observe ≤ 1 is 8.6% . Anecdotally the Fly's Eye event is very close, $\sim 3.0^\circ$, to one of the RXTE sources at RA 88.8° Dec 46.3° and redshift $z=0.02$. If this is a true correlation, then the proton nature of the cosmic ray and/or the measured energy of the cosmic ray are in question.

the AGASA super-GZK events [32].

Additional data would help confirm, or refute, the interesting possibility of highest energy cosmic ray–AGN correlations.

6 Acknowledgements

We wish to acknowledge useful communications with Francesc Ferrer on possible ultra-high energy cosmic rays : BL Lac correlations.

References

- [1] E. Waxman, K. B. Fisher and T. Piran, *Astrophys. J.* **483**, 1 (1997) [astro-ph/9604005]
- [2] A. Cuoco, R. D’Abrusco, G. Longo, G. Miele and P. D. Serpico, *JCAP* 0601 (2006) 009, [astro-ph/0510765]
- [3] K. Dolag, D. Grasso, V. Springel and I. Tkachev, *JCAP* 0501 (2005) 009, [astro-ph/0410419]
- [4] N. Hayashida *et al.*, *Astron. J.* **120**, 2190 (2000), [astro-ph/0008102]
- [5] P. G. Tinyakov and I. I. Tkachev, *JETP Lett.* **74**, 1 (2001), [astro-ph/0102101]
- [6] P. G. Tinyakov and I. I. Tkachev, *JETP Lett.*, **74**, 445 (2001), [astro-ph/0102476]; *Astropart. Phys.*, **18**, 165 (2002), [astro-ph/0111305]
- [7] D. S. Gorbunov, P. G. Tinyakov, I. I. Tkachev and S. V. Troitsky, *Astrophys. J.* **577**, L93 (2002)
- [8] D. S. Gorbunov, P. G. Tinyakov, I. I. Tkachev and S. V. Troitsky, *JETP Lett.*, **80**, 145 (2004) [astro-ph/0406654]
- [9] D. S. Gorbunov and S. V. Troitsky, *Astropart. Phys.* **23**, 175 (2005) [astro-ph/0410741]
- [10] R. U. Abbasi *et al.*, *Astrophys. J.* **636** 680 (2006), [astro-ph/0507120]
- [11] S. L. Dubovsky, P. G. Tinyakov and I. I. Tkachev, *Phys. Rev. Lett.* **85** 1154 (2000), [astro-ph/0001317]
- [12] P. Blasi and D. De Marco, *Astropart. Phys.* **20** 559 (2004), [astro-ph/0307067]
- [13] M. Kachelriess and D. Semikoz, *Astropart. Phys.* **23** 486 (2005) [astro-ph/0405258]

- [14] C. B. Finley and S. Westerhoff, *Astropart. Phys.* **21**, 359 (2004) [astro-ph/0309159]
- [15] S. Westerhoff *et al.*, *Nucl. Phys. B (Proceedings Suppl.)* **136C** 46 (2004), [astro-ph/0408343]; R. U. Abbasi *et al.*, *Astrophys.J.* **623** 164 (2005), [astro-ph/0412617]; S. Westerhoff *et al.*, *Proc. 29th International Cosmic Ray Conference*, **7** 397 (2005), [astro-ph/0507574]
- [16] N. W. Evans, F. Ferrer and S. Sarkar, *Phys. Rev.* **D67** 103005 (2003) [astro-ph/0212533]; *Phys. Rev.* **D69** 128302 (2004) [astro-ph/0403527]
B. Stern and J. Poutanen, *Astrophys.J.* **623** L33 (2005) [astro-ph/0501677]
- [17] G. Sigl, F. Miniati and T. E. Ensslin, [astro-ph/0409098]
- [18] K. Greisen, *Phys. Rev. Lett.* **16**, 748 (1966); G. T. Zatsepin and V. A. Kuzmin, *Pisma Zh. Eksp. Teor. Fiz.* **4**, 144 (1966)
- [19] P. G. Tinyakov and I. I. Tkachev, *Astropart. Phys.* **24** 32 (2005), [astro-ph/0411669]
- [20] M. Kachelriess, P.D. Serpico and M. Teshima, [astro-ph/0510444]
- [21] G. A. Medina Tanco, E. M. de Gouveia Dal Pino and J. E. Horvath, [astro-ph/9707041]
- [22] M. Kachelriess and D. V. Semikoz, [astro-ph/0512498]
- [23] A. Smialkowski, M. Giller and W. Michalak, *J. Phys.* **G28** 1359 (2002), [astro-ph/0203337]
- [24] S. Singh, C-P. Ma, and J. Arons, *Phys. Rev.* **D69** 063003 (2004), [astro-ph/0308257]
- [25] V. Berezhinsky, A.Z. Gazizov and S.I. Grigorieva, [hep-ph/0107306] and [hep-ph/0204357]
- [26] S. Yu. Sazonov and M. G. Revnivtsev, *Astronomy & Astrophysics* **423** 469 (2004), [astro-ph/0402415]; M. Revnivtsev, S. Sazonov, E. Churazov and S. Trudolyubov, [astro-ph/0511444]
- [27] M. Revnivtsev, S. Sazonov, K. Jahoda and M. Gilfanov, *Astronomy & Astrophysics* **418**, 927 (2004)
- [28] V. Berezhinski, A. Gazizov and S. Grigorieva, [astro-ph/0302483]
- [29] A. T. Steffen *et al.*, *Astrophys. J.* **596**, L23 (2003) [astro-ph/0308238]
- [30] A. J. Barger *et al.*, *Astron. J.* **129** 578 (2005), [astro-ph/0410527]
- [31] G. R. Farrar, [astro-ph/0501388]
- [32] www-akeno.icrr.u-tokyo.ac.jp/AGASA/results.html#100EeV
- [33] D.J. Bird, *et al.*, *Astrophys. J.* **441** 144 (1995)